On The Physical Layer Network Coded LDPC Codes for A Multiple-Access Relaying System

Jun Li*, Zihuai Lin*, Jin Xu†, Branka Vucetic*
*School of Electrical and Information Engineering, The University of Sydney, NSW, 2006, AUSTRALIA
Email:{jun.li,zihuai.lin,branka.vucetic}@sydney.edu.au
†Wireless Technology Pre-research Department, Product R&D System, ZTE, Shenzhen, 518055, P.R.CHINA
Email:xu.jin7@zte.com.cn

***Abstract*—In this paper we propose a novel network coded LDPC code design for a multiple-access relay channel (MARC). We first investigate the achievable rate region for the MARC. Then we propose a novel physical layer network coded (PNC) LDPC code structure, named PNC-LDPC code. Next, an iterative detection-and-decoding receiver is designed to deal with the multi-user interference at the destination. Based on the code structure and the iterative receiver, we optimize the degree distribution of the PNC-LDPC code to approach the system achievable rate by utilizing the extrinsic mutual information transfer (EXIT) chart. Simulations show that the performance of our PNC-LDPC code, with a code length of 10000, at the destination, is 1.5 dB away from the capacity.**

I. Introduction

In wireless multiple access relay channels (MARC) with multiple sources, one relay, and one destination, the sources transmit signals to the destination with the help of the relay. Conventional decode-and-forward (DF) protocols of the classic triangle cooperative channels [1] can be readily extended to the MARC. The capacity outer bound and the achievable rate region of the MARC with the DF protocol have been investigated in [2]. According to [2], the achievable rate region of the MARC is the intersection between the rate region of the source-to-relay multiple access channel (MAC) and the rate region of the source-and-relay-to-destination MAC.

Wireless network coding [3, 4] combined with a powerful channel code, e.g., low-density parity check codes [5, 6], is an effective method to approach the achievable rate of the DF based MARC system [7, 8]. In these combined network-channel coding schemes, the relay explicitly/fully decodes the messages of each source and combines these messages based on the channel code to obtain network coded digits. However, these schemes assume that all the sources' signals are transmitted in orthogonal channels, e.g., time/frequency division multiple access (T/FDMA). In the non-orthogonal MARC where the sources' signals are transmitted in the same time and frequency domains, fully decoding of each source's messages at the relay will degrade the error performance due to the multi-user interference.

Physical-layer network coding (PNC) [9], on the other hand, is proposed in two-way relay channels (TWRC) to enhance the error performance of the source-to-relay MAC. The main advantage of the PNC compared to the full-decoding based network coding (FNC) is that it applies partial decoding at the relay by viewing the source-to-relay MAC as a single link channel. This partial decoding of the PNC enables the collaboration of the two sources' signals rather than treating one source's signals as interferences to the other. Simulations in [9] show that the PNC achieves a better error performance relative to the FNC at the relay. This inspiring result motivates us to focus on the applications of the PNC in the MARC.

In this paper we focus on a non-orthogonal MARC network with two sources, one half-duplexing relay and one destination. We consider a strong interference scenario at the relay, i.e., the received signal-to-noise ratios (SNR) of the two sources at the relay are the same. In this scenario, the PNC outperforms the FNC by avoiding fully decoding at the relay. We are interested in the joint design of the PNC and LDPC (PNC-LDPC) code for the MARC with additive white Gaussian noise (AWGN) channels. We first investigate the achievable rate region of the MARC. Then we propose a novel PNC-LDPC code based on the multi-edge type LDPC code structure [6]. Next, an iterative detection-and-decoding receiver is designed to deal with the multi-user interference at the destination. Based on the code structure and the iterative receiver, we optimize the degree distribution of the PNC-LDPC code to approach the system achievable rate by utilizing the extrinsic mutual information transfer (EXIT) chart. Simulations show that the bit error rate (BER) performance of our PNC-LDPC code at the destination is 1.5 dB away from the capacity. Also, the PNC-LDPC code outperforms the FNC based LDPC code by 0.8 dB.

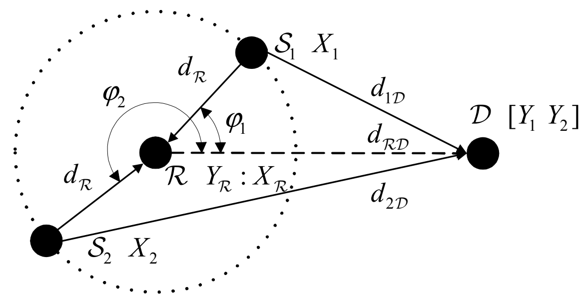

Fig. 1. The system model of the MARC with two-source, one-relay, and one-destination.

This research work is supported by Australian Research Council under Grant No. $DP120100405$, $LP110100110$ and the University of Sydney bridging support grant.

II. System Model

We consider a non-orthogonal MARC network with two sources, one relay and one destination, as shown in Fig. 1. The two sources $\mathcal{S}_1$, $\mathcal{S}_2$ transmit their information to the destination $\mathcal{D}$ with the help of a half-duplexing relay $\mathcal{R}$. We assume that the two sources have the same distance to the relay, and have different ones to the destination. The sources are located in a circle around the relay with the angles φ_1 and φ_2 ($\varphi_1, \varphi_2 \in (0, 2\pi]$), respectively. The distance between $\mathcal{S}_i$ $(i = 1, 2)$ and the relay $\mathcal{R}$ is denoted by $d_{\mathcal{R}}$, the distance between the relay $\mathcal{R}$ and the destination $\mathcal{D}$ is $d_{\mathcal{RD}}$, and the distance between $\mathcal{S}_i$ and the destination $\mathcal{D}$ is $d_{i\mathcal{D}}$, where $d_{1\mathcal{D}} \neq d_{2\mathcal{D}}$. The path losses of all the channels are related to their distances with the same attenuation exponent γ. Therefore, the channel coefficients between $\mathcal{S}_i$ and $\mathcal{R}$, $\mathcal{S}_i$ and $\mathcal{D}$, $\mathcal{R}$ and $\mathcal{D}$ are calculated as $h_{\mathcal{R}} = 1/\sqrt{(d_{\mathcal{R}})^{\gamma}}$, $h_{i\mathcal{D}} = 1/\sqrt{(d_{i\mathcal{D}})^{\gamma}}$, and $h_{\mathcal{RD}} = 1/\sqrt{(d_{\mathcal{RD}})^{\gamma}}$, respectively.

We split one transmission period (n time slots) into two phases. The first phase has tn time slots ($0 < t < 1$, and tn is an integer), in which the two sources simultaneously broadcast their channel encoded codewords X_i to both the destination and the relay. The second phase has $(1-t)n$ time slots, in which the two sources keep silent, while the relay generates the network-coded parity checks for the two sources, encodes these checks by using a channel code and forwards the codeword $X_{\mathcal{R}}$ to the destination. In the first phase, the signal vectors received by the destination and the relay are denoted by Y_1 and $Y_{\mathcal{R}}$, respectively, while in the second phase, the signal vector received at the destination is denoted by Y_2.

We assume that the transmitted codewords X_i, $i = 1, 2$ and $X_{\mathcal{R}}$ are BPSK modulated. We have $X_i = [x_i^1, \cdots, x_i^{tn}]^T$, where x_i^j, $j = 1, \cdots, tn$ is a BPSK symbol, and $X_{\mathcal{R}} = [x_{\mathcal{R}}^1, \cdots, x_{\mathcal{R}}^{(1-t)n}]^T$, where $x_{\mathcal{R}}^{j'}$, $j' = 1, \cdots, (1-t)n$ is a BPSK symbol. Suppose that all the information is encoded by systematic linear channel codes. The information part of X_i is denoted by $\bar{X}_i = [x_i^1, \cdots, x_i^{tnR_i}]^T$, where R_i is $\mathcal{S}_i$'s code rate. The information part of $X_{\mathcal{R}}$ is denoted by $\bar{X}_{\mathcal{R}} = [x_{\mathcal{R}}^1, \cdots, x_{\mathcal{R}}^{(1-t)nR_{\mathcal{R}}}]^T$, where $R_{\mathcal{R}}$ is the relay's code rate. All the noises are modeled as AWGN distributed with a zero mean and variance σ^2. To make the total power constant, we assume that each source has the same power one and the relay has the transmission power of two, i.e., $x_i^j \in \{\pm 1\}$ and $x_{\mathcal{R}}^{j'} \in \{\pm 2\}$. The received signal vectors are expressed as $Y_{\mathcal{R}} = h_{\mathcal{R}}(X_1 + X_2) + N_{\mathcal{R}}$, $Y_1 = h_{1\mathcal{D}}X_1 + h_{2\mathcal{D}}X_2 + N_1$, and $Y_2 = h_{\mathcal{RD}}X_{\mathcal{R}} + N_2$, where $N_{\mathcal{R}}$ is the noise vector observed by the relay, N_1 and N_2 are the noise vectors observed by the destination in the first and second phases, respectively.

III. Achievable Rate Analysis

We now consider the achievable rates of the BIAWGN MARC network with the FNC and the PNC schemes. In the FNC, the relay needs to fully decode two source's information. According to [2], the achievable rate region of the DF based MARC is the intersection between the rate region of the source-to-relay MAC and the rate region of the source-and-relay-to-destination MAC. Then the achievable rate region of the network with the FNC scheme can be written as

$$R_1^{FNC} \leq \frac{\min\{I(X_1; Y_{\mathcal{R}}|X_2), I(X_1; Y_1|X_2) + I(X_{\mathcal{R}}; Y_2)\}}{n},$$
$$R_2^{FNC} \leq \frac{\min\{I(X_2; Y_{\mathcal{R}}|X_1), I(X_2; Y_1|X_1) + I(X_{\mathcal{R}}; Y_2)\}}{n},$$
$$R^{FNC} \leq \frac{\min\{I(X_1, X_2; Y_{\mathcal{R}}), I(X_1, X_2; Y_1) + I(X_{\mathcal{R}}; Y_2)\}}{n}.$$

Next, we study the achievable region in the PNC and first focus on the source-to-relay MAC in the PNC. The relay decodes the superimposed signal $X_1 + X_2$ as a non-binary linear code (on the condition that X_1 and X_2 are generated from the same codebook) rather than fully decodes X_1 and X_2 as that in the FNC [9]. We begin with the mutual information $I(X_1 + X_2; Y_{\mathcal{R}})$. Each symbol in $X_1 + X_2$ can be $-2, 0$ or 2, i.e., $x_1^j + x_2^j \in \{-2, 0, 2\}$. Then the source-to-relay MAC becomes a single link ternary input AWGN channel. Since we have the following probabilities: $P(x_1^j + x_2^j = -2) = 0.25$, $P(x_1^j + x_2^j = 0) = 0.5$, and $P(x_1^j + x_2^j = 2) = 0.25$, the achievable rate of the ternary input AWGN channel can be calculated as

$$I(x_1^j + x_2^j; y_{\mathcal{R}}^j) = \sum_{w=-2,0,2} \int_{-\infty}^{\infty} P(x_1^j + x_2^j = w) p(y_{\mathcal{R}}^j | x_1^j + x_2^j = w) \cdot \log \frac{4p(y_{\mathcal{R}}^j | x_1^j + x_2^j = w)\, \mathrm{d}y_{\mathcal{R}}^j}{p(y_{\mathcal{R}}^j | x_1^j + x_2^j = \pm 2) + 2p(y_{\mathcal{R}}^j | x_1^j + x_2^j = 0)}, \quad (1)$$

where the conditional PDF $p(y_{\mathcal{R}}^j | x_1^j + x_2^j)$ is

$$p(y_{\mathcal{R}}^j | x_1^j + x_2^j) = \frac{1}{\sqrt{2\pi}\sigma} \exp\left\{ -\frac{(y_{\mathcal{R}}^j - h_{\mathcal{R}}(x_1^j + x_2^j))^2}{2\sigma^2} \right\}. \quad (2)$$

We calculate the entropy of each ternary symbol $x_1^j + x_2^j$ as $H(x_1^j + x_2^j) = -0.25 \log 0.25 - 0.5 \log 0.5 - 0.25 \log 0.25 = 1.5$(bit). Note that $I(x_1^j + x_2^j; y_{\mathcal{R}}^j)$ is the achievable rate of the source-to-relay ternary input AWGN channel. According to the property of PNC [9], the achievable rate of each source in the source-to-relay MAC can be calculated as $I(x_1^j + x_2^j; y_{\mathcal{R}}^j)/H(x_1^j + x_2^j)$. We have $I(x_1^j + x_2^j; y_{\mathcal{R}}^j) = I(x_1^j, x_2^j; y_{\mathcal{R}}^j)$. Therefore in the source-to-relay MAC, each source can transmit with the maximum rate $\frac{2}{3}I(x_1^j, x_2^j; y_{\mathcal{R}}^j)$ in the same time. Then the achievable sum rate of the source-to-destination MAC is $\frac{4}{3}I(x_1^j, x_2^j; y_{\mathcal{R}}^j)$. Also note that the achievable rate region of the source-and-relay-to-destination MAC of the PNC and the FNC are the same. We thus have the achievable rate region for the PNC as

$$R_1^{PNC} \leq \frac{\min\left\{\frac{2}{3}I(X_1, X_2; Y_{\mathcal{R}}), I(X_1; Y_1|X_2) + I(X_{\mathcal{R}}; Y_2)\right\}}{n},$$
$$R_2^{PNC} \leq \frac{\min\left\{\frac{2}{3}I(X_1, X_2; Y_{\mathcal{R}}), I(X_2; Y_1|X_1) + I(X_{\mathcal{R}}; Y_2)\right\}}{n},$$
$$R^{PNC} \leq \frac{\min\left\{\frac{4}{3}I(X_1, X_2; Y_{\mathcal{R}}), I(X_1, X_2; Y_1) + I(X_{\mathcal{R}}; Y_2)\right\}}{n}.$$

IV. Structure of PNC-LDPC Codes

In the PNC, the relay firstly decodes X_1+X_2 from $Y_{\mathcal{R}}$ and maps X_1+X_2 to the element-wise product of X_1 and X_2, i.e., X_1X_2 [9]. Then the relay generates the network coded parity check digits $\bar{X}_{\mathcal{R}}$ based on X_1X_2 and encodes $\bar{X}_{\mathcal{R}}$ into the codeword $X_{\mathcal{R}}$. The destination firstly decodes $X_{\mathcal{R}}$ from Y_2 and then decodes the two sources's information based on Y_1 and $X_{\mathcal{R}}$. We assume that $\bar{X}_{\mathcal{R}}$ can be perfectly decoded from Y_2 at the destination.

The source $\mathcal{S}_1$ is encoded by a single link LDPC code with code rate R_1, which is denoted by $\mathbb{C}_1$. The source $\mathcal{S}_2$ is encoded by another LDPC code $\mathbb{C}_2$ with code rate R_2. Without loss of generality, we assume $R_2 < R_1$. Since in the PNC, both sources must possess the same code, we design the code $\mathbb{C}_2$ to be a sub-code of $\mathbb{C}_1$. More specifically, $\mathbb{C}_2$ is designed to be rate compatible, which can be seen as a concatenated code $(\mathbb{C}_{out}, \mathbb{C}_{in})$. We set $\mathbb{C}_{in} = \mathbb{C}_1$. The information of $\mathcal{S}_2$ is firstly encoded by the outer code $\mathbb{C}_{out}$ with rate $\frac{R_2}{R_1}$, and then the output of $\mathbb{C}_{out}$ is encoded by the inner code $\mathbb{C}_1$ (with rate R_1). We denote the parity check matrix of $\mathbb{C}_{out}$ and $\mathbb{C}_1$ as $\mathbf{H}_{out}$ and $\mathbf{H}_1$, respectively. Then the parity check matrix $\mathbf{H}_2$ of $\mathbb{C}_2$ can be expressed as

$$\mathbf{H}_2 = \begin{bmatrix} \mathbf{H}_{out} \quad \mathbf{O} \\ ------- \\ \leftarrow \ \mathbf{H}_1 \ \rightarrow \end{bmatrix}, \tag{3}$$

where $\mathbf{O}$ is a zero matrix, and $\mathbf{H}_1$, $\mathbf{H}_2$, $\mathbf{H}_{out}$ and $\mathbf{O}$ have the size $nt(1-R_1)\times nt$, $nt(1-R_2)\times nt$, $nt(R_1-R_2)\times ntR_1$ and $nt(R_1-R_2)\times nt(1-R_1)$, respectively.

At the relay, X_1+X_2 is viewed as a codeword of a non-binary code which is derived from $\mathbb{C}_1$, and $\mathcal{S}_2$'s outer code $\mathbb{C}_{out}$ is transparent to the relay. The relay generates the network coded symbols $\bar{X}_{\mathcal{R}}$ from X_1X_2 based on a matrix $\mathbf{H}_{\mathcal{R}}$, i.e., $\bar{X}_{\mathcal{R}} = \mathbf{H}_{\mathcal{R}}(X_1X_2)$. The information symbols in $\bar{X}_{\mathcal{R}}$ are then encoded by a desired channel code to the codeword $X_{\mathcal{R}}$. The lengths of $\bar{X}_{\mathcal{R}}$ and $X_{\mathcal{R}}$ are $(1-t)nR_{\mathcal{R}}$ and $(1-t)n$, respectively. The size of $\mathbf{H}_{\mathcal{R}}$ is $(1-t)nR_{\mathcal{R}}\times nt$. At the destination, the symbols in $\bar{X}_{\mathcal{R}}$ are firstly decoded. The code at the destination is designed by viewing $[X_1\ X_2\ \bar{X}_{\mathcal{R}}]^T$ as its codeword, with its parity check matrix denoted by $\mathbf{H}_{\mathcal{D}}$.

Fig. 2(a) shows the structure of the parity check matrix $\mathbf{H}_{\mathcal{D}}$. In Fig. 2(a), the sub-matrices $\mathbf{O}_1$, $\mathbf{O}_2$, $\mathbf{O}_3$ and $\mathbf{O}_4$ are four zero matrices, $\mathbf{I}$ is an identity matrix. The size of $\mathbf{O}_1$ is $nt(1-R_1)\times nt$, the size of $\mathbf{O}_2$ is $nt(1-R_1)\times(1-t)nR_{\mathcal{R}}$, the size of $\mathbf{O}_3$ is $nt(1-R_2)\times nt$, and the size of $\mathbf{O}_4$ is $nt(1-R_2)\times(1-t)nR_{\mathcal{R}}$. The sub-matrix $[\mathbf{H}_{\mathcal{R}}\ \mathbf{H}_{\mathcal{R}}]$ of $\mathbf{H}_{\mathcal{D}}$ corresponds to the network coding at the relay. We denote the code that corresponds to the sub-matrix $[\mathbf{H}_{\mathcal{R}}\ \mathbf{H}_{\mathcal{R}}]$ of $\mathbf{H}_{\mathcal{D}}$ as $\mathbb{C}_{\mathcal{R}}$, denote the code that corresponds to the left matrix $\mathbf{H}_{\mathcal{R}}$ of $[\mathbf{H}_{\mathcal{R}}\ \mathbf{H}_{\mathcal{R}}]$ as $\mathbb{C}_{\mathcal{R},1}$, and denote the code that corresponds to the right matrix $\mathbf{H}_{\mathcal{R}}$ of $[\mathbf{H}_{\mathcal{R}}\ \mathbf{H}_{\mathcal{R}}]$ as $\mathbb{C}_{\mathcal{R},2}$.

We utilize multi-edge type structure [6] to represent the code structure at the destination. The multi-edge type ensemble can be specified through two polynomials, one is associated with variable nodes, and the other is associated with check nodes. The polynomials are given by $v(\mathbf{r},\mathbf{w}) = \sum v_{\mathbf{b},\mathbf{d}}\mathbf{r}^{\mathbf{b}}\mathbf{w}^{\mathbf{d}}$,

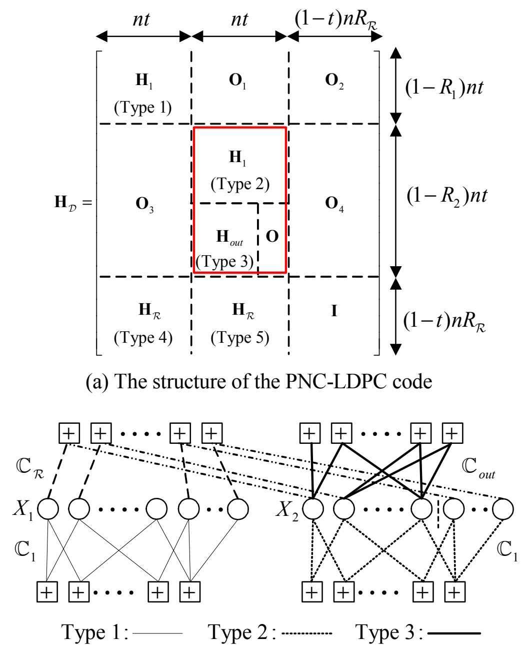

(a) The structure of the PNC-LDPC code

(b) Tanner graph of the PNC-LDPC code

Fig. 2. Multi-edge type structure of the PNC-LDPC code.

and $\mu(\mathbf{w}) = \sum \mu_{\mathbf{d}}\mathbf{w}^{\mathbf{d}}$, where $\mathbf{d} = [d_1, d_2, \cdots, d_{n_\varsigma}]$ is the *edge degree vector* (EDV) of length n_ς and $\mathbf{b} = [b_0, b_1, \cdots, b_{n_\tau}]$ is the *received degree vector* (RDV) of length $n_\tau+1$. The vector of variables is denoted by $\mathbf{w} = [w_1, \cdots, w_{n_\varsigma}]$, while $\mathbf{r} = [r_0, r_1, \cdots, r_{n_\tau}]$ denotes the vector of variables corresponding to the received distributions. Here, we have $\mathbf{w}^{\mathbf{d}} = \prod_{\iota=1}^{n_\varsigma} w_\iota^{d_\iota}$ and $\mathbf{r}^{\mathbf{b}} = \prod_{\iota=0}^{n_\tau} r_\iota^{b_\iota}$. The coefficients $v_{\mathbf{b},\mathbf{d}}$ and $\mu_{\mathbf{d}}$ correspond to the percentage of variable nodes with type ($\mathbf{b}$, $\mathbf{d}$) and check nodes with type ($\mathbf{d}$), respectively.

Fig. 2 (b) shows the Tanner Graph of the PNC-LDPC code represented by a multi-edge type code structure. The symbols of $\bar{X}_{\mathcal{R}}$ are neglected since $\bar{X}_{\mathcal{R}}$ has been successfully decoded at the destination. We denote the five edge types as Type 1, Type 2, Type 3, Type 4, and Type 5, corresponding to the codes $\mathbb{C}_1$, $\mathbb{C}_1$ (the inner code of $\mathbb{C}_2$), $\mathbb{C}_{out}$, $\mathbb{C}_{\mathcal{R},1}$, and $\mathbb{C}_{\mathcal{R},2}$, respectively. Next, we assign the structure of the PNC-LDPC code with two types of the received degree (i.e., $n_\tau = 2$), since the codewords X_1 and X_2 experience two different signal-to-interference-noise ratio. With five different edge-types and two types of received degree in $\mathbf{H}_{\mathcal{R}}$, the polynomials for $\mathbf{H}_{\mathcal{D}}$ can be written as $v(\mathbf{r},\mathbf{w}) = r_1\sum_{a=1}^{d_{v,1}}\sum_{d=0}^{d_{v,4}} v_{[0,1,0],[a,0,0,d,0]}w_1^a w_4^d + r_2\sum_{b=1}^{d_{v,2}}\sum_{c=0}^{d_{v,3}}\sum_{e=0}^{d_{v,5}} v_{[0,0,1],[0,b,c,0,e]}w_2^b w_3^c w_5^d$, and $\mu(\mathbf{w}) = \sum_{a=1}^{d_{c,1}} \mu_{[a,0,0,0,0]}w_1^a + \sum_{b=1}^{d_{c,2}}\mu_{[0,b,0,0,0]}w_2^b + \sum_{c=1}^{d_{c,3}}\mu_{[0,0,c,0,0]}w_3^c + \sum_{d=1}^{d_{c,4}}\mu_{[0,0,0,d,0]}w_4^d + \sum_{e=1}^{d_{c,5}}\mu_{[0,0,0,0,e]}w_5^d$, where r_1 and r_2 denote

$$l_{\text{dec}}^{\text{mud}}(x_1^j) = \ln\left(\frac{p(y_1^j|x_1^j=1,x_2^j=1)P(x_1^j=1)P(x_2^j=1)+p(y_1^j|x_1^j=1,x_2^j=-1)P(x_1^j=1)P(x_2^j=-1)}{p(y_1^j|x_1^j=-1,x_2^j=1)P(x_1^j=-1)P(x_2^j=1)+p(y_1^j|x_1^j=-1,x_2^j=-1)P(x_1^j=-1)P(x_2^j=-1)}\right) \quad (4)$$

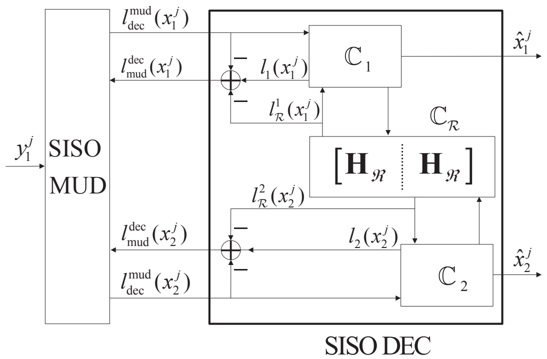

Fig. 3. Iterative receiver structure at the destination.

the variable nodes associated with X_1 and X_2, respectively. More specifically, r_1 and r_2 are associated with the $\mathcal{S}_1$-to-destination channel and the $\mathcal{S}_2$-to-destination channel, respectively. The variable nodes transmitted in the $\mathcal{S}_1$-to-destination channel (i.e., the symbols in X_1) are connected to the edges of Type 1 and Type 4, while the variable nodes transmitted in the $\mathcal{S}_2$-to-destination channel (i.e., the symbols in X_2) are connected to the edges of Type 2, Type 3 and Type 5. The EDV $\mathbf{d} = [a, b, c, d, e]$ represents five types of edge degree with a, b, c, d and e denoting the variable or check node' degrees of Type 1, Type 2, Type 3, Type 4, and Type 5, respectively. In the design of the PNC-LDPC code, we first optimize the single-link LDPC code $\mathbb{C}_1$ according to $\mathcal{S}_1$'s code rate. Then based on both $\mathbb{C}_1$ and the multiuser detector at the destination, we jointly optimize $\mathbb{C}_{out}$ and $\mathbb{C}_{\mathcal{R}}$.

V. Receiver Structure and Code Optimization

A. Iterative Receiver

The iterative receiver structure is shown in Fig. 3. There is a soft-in-soft-out (SISO) multiuser detector (denoted by MUD), and an SISO belief propagation (BP) decoder (denoted by DEC). Recall that the parity check matrix of the DEC, i.e., $\mathbf{H}_{\mathcal{D}}$, is composed of $\mathbf{H}_1$ (corresponds to the code $\mathbb{C}_1$), $\mathbf{H}_2$ (corresponds to the code $\mathbb{C}_2$), and $[\mathbf{H}_{\mathcal{R}}\ \mathbf{H}_{\mathcal{R}}]$ (corresponds to the code $\mathbb{C}_{\mathcal{R}}$). The extrinsic log-likelihood ratios (LLR), i.e., $l_{\text{dec}}^{\text{mud}}(x_i^j)$ and $l_{\text{mud}}^{\text{dec}}(x_i^j)$ are exchanged between the MUD and the DEC in each iteration. The MUD utilizes the input LLR $l_{\text{mud}}^{\text{dec}}(x_i^j)$ to update its output LLR $l_{\text{dec}}^{\text{mud}}(x_i^j)$. The *a priori* LLR $l_{\text{mud}}^{\text{dec}}(x_i^j)$ is defined as $\ln(P(x_i^j = 1)/(x_i^j = -1))$. Without loss of generality, we focus on the LLR $l_{\text{dec}}^{\text{mud}}(x_1^j)$, which can be expressed in Equation (4).

In the MUD, we use the extrinsic LLR $l_{\text{mud}}^{\text{dec}}(x_2^j)$ to update the probability $P(x_2^j)$ in $l_{\text{dec}}^{\text{mud}}(x_1^j)$ and use the extrinsic LLR $l_{\text{mud}}^{\text{dec}}(x_1^j)$ to update the probability $P(x_1^j)$ in $l_{\text{dec}}^{\text{mud}}(x_2^j)$ in each iteration. The probability $P(x_i^j)$ is updated as $P(x_i^j = 1) = \frac{\exp(l_{\text{mud}}^{\text{dec}}(x_i^j))}{1+\exp(l_{\text{mud}}^{\text{dec}}(x_i^j))}$, and $P(x_i^j = -1) = \frac{1}{1+\exp(l_{\text{mud}}^{\text{dec}}(x_i^j))}$.

From the DEC point of view, $l_{\text{dec}}^{\text{mud}}(x_1^j)$ and $l_{\text{dec}}^{\text{mud}}(x_2^j)$ are utilized as the extrinsic channel LLRs. BP decoding is applied to the parity check matrix $\mathbf{H}_{\mathcal{D}}$. The DEC structure is shown in Fig. 3. We can see that, joint decoding of the two sources' codewords is enabled by the sub-matrix $[\mathbf{H}_{\mathcal{R}}\ \mathbf{H}_{\mathcal{R}}]$ in the parity check matrix $\mathbf{H}_{\mathcal{D}}$. We denote the output LLR of the code $\mathbb{C}_i$ as $l_i(x_i^j)$, and the output LLR from $\mathbb{C}_{\mathcal{R}}$ to $\mathbb{C}_i$ as $l_{\mathcal{R}}^i(x_i^j)$. From the code structure of $\mathbb{C}_{\mathcal{R}}$, we can see that the LLR $l_{\mathcal{R}}^1(x_1^j)$ is dependent on the information from $\mathbb{C}_2$ and $l_{\mathcal{R}}^2(x_2^j)$ is dependent on the information from $\mathbb{C}_1$. To make the output LLR of the DEC, i.e., $l_{\text{mud}}^{\text{dec}}(x_i^j)$ to be extrinsic, we calculate it as $l_{\text{mud}}^{\text{dec}}(x_i^j) = l_i(x_i^j) - l_{\text{dec}}^{\text{mud}}(x_i^j) - l_{\mathcal{R}}^i(x_i^j)$.

B. Code Optimization

Now, we focus on the optimization of the PNC-LDPC code. We first optimize the code $\mathbb{C}_1$ as a single link ternary LDPC code, which guarantees a good decoding performance of $X_1 + X_2$ at the relay. The optimization can follow a method similar to the one in [9]. Then based on $\mathbb{C}_1$ and the iterative receiver, we jointly optimize $\mathbb{C}_{out}$ and $\mathbb{C}_{\mathcal{R}}$. We have some constraints on the structures of $\mathbb{C}_{out}$ and $\mathbb{C}_{\mathcal{R}}$. For $\mathbb{C}_{out}$, when we optimize its degree distribution, we should ensure that the sub-matrix in the right-top corner of $\mathbf{H}_2$ is a zero matrix with size $nt(R_1 - R_2) \times nt(1 - R_1)$. For $\mathbb{C}_{\mathcal{R}}$, due to the symmetric structure of the sub-matrix $[\mathbf{H}_{\mathcal{R}}\ \mathbf{H}_{\mathcal{R}}]$, the symbols x_1^j and x_2^j are always connected by the same parity checks in $\mathbb{C}_{\mathcal{R}}$.

The EXIT chart [10] is utilized to optimize $\mathbb{C}_{out}$ and $\mathbb{C}_{\mathcal{R}}$. We optimize the degree distribution of $\mathbb{C}_{out}$ and $\mathbb{C}_{\mathcal{R}}$ by fixing the codes $\mathbb{C}_1$ and the MUD. First, we track the extrinsic mutual information transfer inside of the DEC. We need to find the relationship between the input and the output extrinsic mutual information of the DEC. Since the codeword digits of different sources experience different channel conditions, we average the extrinsic mutual information within each edge type.

To track the extrinsic mutual information inside of the DEC, we denote by $I_{Ev,m}^{(k,q)}$ the average extrinsic mutual information sent on the edges of Type m, $m = 1, 2, 3, 4, 5$ from the variable nodes to the check nodes in the q-th iteration of the BP decoding and the k-th iteration between the MUD and the DEC. We denote by $I_{Ec,m}^{(k,q)}$ the average extrinsic mutual information sent on the edges of Type m from the check nodes to the variable nodes in the q-th iteration of the BP decoding and the k-th iteration between the MUD and the DEC. Also note that the extrinsic mutual information on an edge connecting the variable nodes to the check nodes, at the output of the variable nodes, is the *a-priori* mutual information for the check nodes in the current

$$
\begin{aligned}
I_{Ev,1}^{(k,q)} &= \sum_{a=1}^{d_{v,1}} \sum_{d=1}^{d_{v,4}} J\left(\sqrt{(a-1)\left(J^{-1}\left(I_{Av,1}^{(k,q)}\right)\right)^2 + d\left(J^{-1}\left(I_{Av,4}^{(k,q)}\right)\right)^2 + \left(\sigma_1^{(k)}\right)^2}\right)\lambda_{[a,0,0,d,0]}^{(1)},\\
I_{Ev,2}^{(k,q)} &= \sum_{b=1}^{d_{v,2}} \sum_{c=1}^{d_{v,3}} \sum_{e=1}^{d_{v,5}} J\left(\sqrt{(b-1)\left(J^{-1}\left(I_{Av,2}^{(k,q)}\right)\right)^2 + c\left(J^{-1}\left(I_{Av,3}^{(k,q)}\right)\right) + e\left(J^{-1}\left(I_{Av,5}^{(k,q)}\right)\right)^2 + \left(\sigma_2^{(k)}\right)^2}\right)\lambda_{[0,b,c,0,e]}^{(2)},\\
I_{Ev,3}^{(k,q)} &= \sum_{b=1}^{d_{v,2}} \sum_{c=1}^{d_{v,3}} \sum_{e=1}^{d_{v,5}} J\left(\sqrt{b\left(J^{-1}\left(I_{Av,2}^{(k,q)}\right)\right)^2 + (c-1)\left(J^{-1}\left(I_{Av,3}^{(k,q)}\right)\right) + e\left(J^{-1}\left(I_{Av,5}^{(k,q)}\right)\right)^2 + \left(\sigma_2^{(k)}\right)^2}\right)\lambda_{[0,b,c,0,e]}^{(3)}, \quad (5)\\
I_{Ev,4}^{(k,q)} &= \sum_{a=1}^{d_{v,1}} \sum_{d=1}^{d_{v,4}} J\left(\sqrt{a\left(J^{-1}\left(I_{Av,1}^{(k,q)}\right)\right)^2 + (d-1)\left(J^{-1}\left(I_{Av,4}^{(k,q)}\right)\right)^2 + \left(\sigma_1^{(k)}\right)^2}\right)\lambda_{[a,0,0,d,0]}^{(4)},\\
I_{Ev,5}^{(k,q)} &= \sum_{b=1}^{d_{v,2}} \sum_{c=1}^{d_{v,3}} \sum_{e=1}^{d_{v,5}} J\left(\sqrt{b\left(J^{-1}\left(I_{Av,2}^{(k,q)}\right)\right)^2 + c\left(J^{-1}\left(I_{Av,3}^{(k,q)}\right)\right) + (e-1)\left(J^{-1}\left(I_{Av,5}^{(k,q)}\right)\right)^2 + \left(\sigma_2^{(k)}\right)^2}\right)\lambda_{[0,b,c,0,e]}^{(5)}.
\end{aligned}
$$

iteration of BP decoding, i.e., $I_{Ac,m}^{(k,q)} = I_{Ev,m}^{(k,q)}$. Similarly, the extrinsic mutual information on an edge connecting the check nodes to the variable nodes, at the output of the check node, is the *a-priori* mutual information for the variable nodes in the next iteration of BP decoding, i.e., $I_{Av,m}^{(k,q+1)} = I_{Ec,m}^{(k,q)}$. We use the $J(\cdot)$ function to represent the mutual information of a single link BIAWGN channel, which is derived in [10]. We denote the variance of the LLR $l_{\text{dec}}^{\text{mud}}(x_i^j)$ as $\left(\sigma_i^{(k)}\right)^2$ in the k-th iteration between the MUD and the DEC. According to [10], we have the extrinsic mutual information, at the output of the variable nodes as Equation (5). In (5), the percentages of the edges connected to the variable nodes of different degrees within each edge type are calculated as $\lambda_{[a,0,0,d,0]}^{(1)} = \frac{v_{[0,1,0],[a,0,0,d,0]}a}{\sum_{a'=1}^{d_{v,1}}\sum_{d'=1}^{d_{v,4}} v_{[0,1,0],[a',0,0,d',0]}a'}$, $\lambda_{[0,b,c,0,e]}^{(2)} = \frac{v_{[0,0,1],[0,b,c,0,e]}b}{\sum_{b'=1}^{d_{v,2}}\sum_{c'=1}^{d_{v,3}}\sum_{e'=1}^{d_{v,5}} v_{[0,0,1],[0,b',c',0,e']}b'}$, $\lambda_{[0,b,c,0,e]}^{(3)} = \frac{v_{[0,0,1],[0,b,c,0,e]}c}{\sum_{b'=1}^{d_{v,2}}\sum_{c'=1}^{d_{v,3}}\sum_{e'=1}^{d_{v,5}} v_{[0,0,1],[0,b',c',0,e']}c'}$, $\lambda_{[a,0,0,d,0]}^{(4)} = \frac{v_{[0,1,0],[a,0,0,d,0]}d}{\sum_{a'=1}^{d_{v,1}}\sum_{d'=1}^{d_{v,4}} v_{[0,1,0],[a',0,0,d',0]}d'}$, and $\lambda_{[0,b,c,0,e]}^{(5)} = \frac{v_{[0,0,1],[0,b,c,0,e]}e}{\sum_{b'=1}^{d_{v,2}}\sum_{c'=1}^{d_{v,3}}\sum_{e'=1}^{d_{v,5}} v_{[0,0,1],[0,b',c',0,e']}e'}$.

We have the extrinsic mutual information, at the output of the check nodes as

$$
\begin{aligned}
I_{Ec,1}^{(k,q)} &= 1 - \sum_{a=1}^{d_{c,1}} J\left(\sqrt{(a-1)\left(J^{-1}\left(I_{Ac,1}^{(k,q)}\right)\right)^2}\right)\rho_{[a,0,0,0,0]}^{(1)},\\
I_{Ec,2}^{(k,q)} &= 1 - \sum_{b=1}^{d_{c,2}} J\left(\sqrt{(b-1)\left(J^{-1}\left(I_{Ac,2}^{(k,q)}\right)\right)^2}\right)\rho_{[0,b,0,0,0]}^{(2)},\\
I_{Ec,3}^{(k,q)} &= 1 - \sum_{c=1}^{d_{c,3}} J\left(\sqrt{(c-1)\left(J^{-1}\left(I_{Ac,3}^{(k,q)}\right)\right)^2}\right)\rho_{[0,0,c,0,0]}^{(3)},\\
I_{Ec,4}^{(k,q)} &= 1 - \sum_{d=1}^{d_{c,4}} J\left(\sqrt{(d-1)\left(J^{-1}\left(I_{Ac,4}^{(k,q)}\right)\right)^2}\right)\rho_{[0,0,0,d,0]}^{(4)},\\
I_{Ec,5}^{(k,q)} &= 1 - \sum_{e=1}^{d_{c,5}} J\left(\sqrt{(e-1)\left(J^{-1}\left(I_{Ac,5}^{(k,q)}\right)\right)^2}\right)\rho_{[0,0,0,0,e]}^{(5)},
\end{aligned}
$$

where the percentages of the edges connected to the check nodes of different degrees within each edge type are calculated as $\rho_{[a,0,0,0,0]}^{(1)} = \frac{\mu_{[a,0,0,0,0]}a}{\sum_{a'=1}^{d_{c,1}}\mu_{[a',0,0,0,0]}a'}$, $\rho_{[0,b,0,0,0]}^{(2)} = \frac{\mu_{[0,b,0,0,0]}b}{\sum_{b'=1}^{d_{c,2}}\mu_{[0,b',0,0,0]}b'}$, $\rho_{[0,0,c,0,0]}^{(3)} = \frac{\mu_{[0,0,c,0,0]}c}{\sum_{c'=1}^{d_{c,3}}\mu_{[0,0,c',0,0]}c'}$, $\rho_{[0,0,0,d,0]}^{(4)} = \frac{\mu_{[0,0,0,d,0]}d}{\sum_{d'=1}^{d_{c,4}}\mu_{[0,0,0,d',0]}d'}$, and $\rho_{[0,0,0,0,e]}^{(5)} = \frac{\mu_{[0,0,0,0,e]}e}{\sum_{e'=1}^{d_{c,5}}\mu_{[0,0,0,0,e']}e'}$. We assume the BP decoder performs Q iterations in the DEC. Then at the end of the iterations of the BP decoding, the extrinsic mutual information from the DEC to the MUD, is given by

$$
\begin{aligned}
I_{1,DEC\to MUD}^{(k)} &= \sum_{a=1}^{d_{v,1}} \sum_{d=1}^{d_{v,4}} J\left(\sqrt{a\left(J^{-1}\left(I_{Av,1}^{(k,Q)}\right)\right)^2}\right)\lambda_{[a,0,0,d]}^{(1)},\\
I_{2,DEC\to MUD}^{(k)} &= \sum_{b=1}^{d_{v,2}} \sum_{c=1}^{d_{v,3}} \sum_{d=1}^{d_{v,4}}\\
& J\left(\sqrt{b\left(J^{-1}\left(I_{Av,2}^{(k,Q)}\right)\right)^2 + c\left(J^{-1}\left(I_{Av,3}^{(k,Q)}\right)\right)}\right)\lambda_{[0,b,c,d]}^{(2)}.
\end{aligned}
$$

We assume that the receiver at the destination conducts total K iterations between the MUD and the DEC. At the end of the K iterations, we ensure that $I_{i,DEC\to MUD}^{(K)} \to 1$. Given these requirements, we optimize the code by searching a code profile with the maximum threshold σ.

VI. Simulations

In the simulations, we consider the following asymmetric MARC network. We assume that $\varphi_1 = \frac{\pi}{2}$, $\varphi_2 = \pi$, $d_{\mathcal{R}} = 0.5$, $d_{\mathcal{RD}} = 0.5$, $d_{1\mathcal{D}} = \sqrt{0.5^2 + 0.5^2} = 0.7071$, and $d_{2\mathcal{D}} = 0.5 + 0.5 = 1.0$. The channel attenuation exponents of all the channels are the same and equal to $\gamma = 2$. The SNR is defined as the transmission SNR of each source, i.e., $\frac{1}{\sigma^2}$. Fig. 4 shows the optimized achievable rates of the MARC network. The achievable rates of the MARC network are optimized based on time allocation. From Fig. 4, the achievable rates of the MARC with the PNC are always larger than the FNC.

We set $n = 10000$ in the BER simulations. We design a LDPC code for the FNC, which is denoted by FNC-LDPC

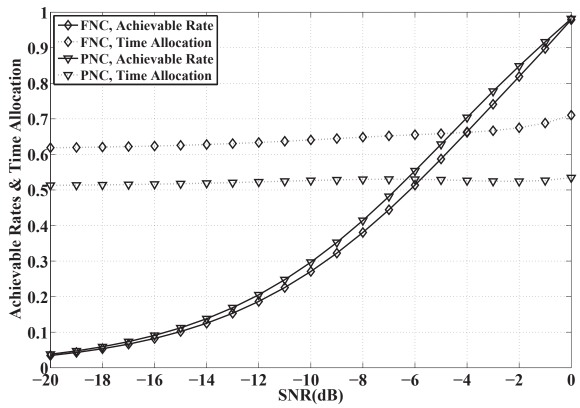

Fig. 4. Optimal time allocations and achievable rates of the MARC with the FNC and the PNC schemes.

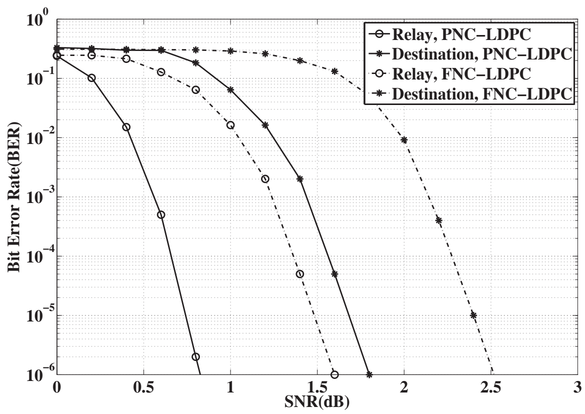

Fig. 5. BER curves for PNC-LDPC and FNC-LDPC.

code. We use the FNC-LDPC code as a benchmark of the PNC-LDPC code. To have a fair comparison of the two codes, we set the PNC and the FNC to have the same achievable rate. Without loss of generality, we design the codes at the SNR of 0 dB. We determine the code rates for both the PNC-LDPC code and the FNC-LDPC code as follows. First, we choose the code rates $R_1 = 0.8$ and $R_2 = 0.59$ for the codeword X_1 and X_2, respectively. The sum rate $R_1 + R_2 = 1.39$, which is slightly smaller than the achievable sum rate of the source-to-relay MAC, i.e., 1.33. Second, in the relay-to-destination channel, we choose relay's code rate $R_{\mathcal{R}}$ as $R_{\mathcal{R}} = I(x^j_{\mathcal{R}}; y^j_2) = 0.99$. The extra rate provided by the relay (relative to the codeword length) is calculated as $\frac{1-t^{FNC}}{t^{FNC}} R_{\mathcal{R}} = 0.4$. At the destination, the equivalent sum code rate of the two sources is $1.39-0.4 = 0.99$, which equals the achievable rate of the MARC network at 0 dB (See Fig. 4).

Next, we shall optimize the codes based on both the code structure and the receiver structure at the destination. In the design of FNC-LDPC code, we optimize the codes $\mathbb{C}_{1,FNC}$, $\mathbb{C}_{2,FNC}$ and $\mathbb{C}_{\mathcal{R},FNC}$ for $\mathcal{S}_1$, $\mathcal{S}_2$, and $\mathcal{R}$, respectively. Each of $\mathbb{C}_{1,FNC}$ and $\mathbb{C}_{2,FNC}$ is designed to be good codes in point-to-point channels and $\mathbb{C}_{\mathcal{R},FNC}$ is optimized according to the degree distributions of $\mathbb{C}_{1,FNCl}$ and $\mathbb{C}_{2,FNC}$. For the PNC-LDPC code, we optimize the code by following the method in Section V. The code profiles of the WNC-LDPC and PNC-LDPC codes are omitted due to page limit, which are shown in the journal version of this work. Fig. 5 shows the BER curves of two coding schemes. Note that in the figure, the 'Relay' means the BER at the relay, and the 'Destination' means the BER at the destination. First, we investigate the decoding performance at the relay. From Fig. 5 we can see that, in the FNC, because the relay has to fully decode two sources' information, the decoding performance is much worse than that of the PNC at the relay. Then we focus on the decoding performance at the destination. We can see that the performance of the proposed PNC-LDPC is about 1.5 dB away from the capacity (at BER 10^{-4}). Also, our PNC-LDPC code is about 0.8 dB better compared with the FNC-LDPC code.

VII. Conclusion

In this paper we propose a PNC-LDPC code structure based on the multi-edge type LDPC codes for a MARC network. An iterative detection-and-decoding receiver is designed to deal with the multi-user interference at the destination. We optimize the PNC-LDPC code to approach the achievable rates by utilizing the EXIT chart of the iterative detection-and-decoding receiver. Numerical results show that the achievable rates of the MARC with the PNC are always larger than that with the FNC. In the BER simulations, the BER performance of our PNC-LDPC code is only 1.5 dB away from the capacity. Also, relative to the LDPC code optimized for the FNC, the PNC-LDPC code has a gain of 0.8 dB gain.

References

[1] A. Sendonaris, E. Erkip, and B. Azhang, "User cooperation diversity - Part I: system description," *IEEE Transactions on Communications*, vol. 51, no. 11, pp. 1927-1938, Nov. 2003.

[2] L. Sankar, N. B. Mandayam, and H. V. Poor, "On the sum-capacity of degraded Gaussian multiple-access relay channels," *IEEE Transactions on Information Theory*, vol. 55, no. 12, pp. 5394-5411, Dec. 2009.

[3] J. Li, J. Yuan, R. Malaney, M. Xiao, and W. Chen, "Full-Diversity Binary Frame-Wise Network Coding for Multiple-Source Multiple-Relay Networks over Slow Fading Channels," *IEEE Transactions on Vehicular Technology*, vol. 61, no. 3, pp. 1346-1360, Mar. 2012.

[4] M. Xiao and M. Skoglund, "Multiple-user cooperative communications based on linear network coding," *IEEE Transactions on Communications*, vol. 58, no. 12, pp. 3345-3351, Dec. 2010.

[5] T. J. Richardson, M. A. Shokrollahi, and R. L. Urbanke, "Design of capacity-approaching irregular LDPC codes," *IEEE Transactions on Information Theory*, vol. 47, no. 2, pp. 619-637, Feb. 2001.

[6] T. J. Richardson and R. L. Urbanke, "Multi-edge type LDPC codes," Available Online: http://lthcwww.epfl.ch/papers/mutiledge.ps.

[7] J. Li, J. Yuan, R. Malaney, Marwan H. Azmi, and M. Xiao, "Network coded LDPC code design for a multi-source relaying system," *IEEE Transactions on Wireless Communications*, vol. 10, no. 5, pp. 1538-1551, May 2011.

[8] K. Pang, Z. Lin, Y. Li and B. Vucetic, "Joint Network-Channel Code Design for Real Wireless Relay Networks", *6th International Symposium on Turbo Codes and Iterative Information Processing*, Sept. 2010.

[9] S. Zhang and S.-C. Liew, "Channel coding and decoding in relay system operated with physical-layer network coding," *IEEE Journal on Selected Areas in Communications*, vol. 27, no. 5, pp. 778-796, Jun. 2009.

[10] S. Brink, "Convergence behavior of iteratively decoded parallel concatenated codes," *IEEE Transactions on Communications*, vol. 49, no. 10, pp. 1727-1737, Oct. 2001.